JOURNAL OF AIRCRAFT
Vol. 36, No. 2, March–April 1999

Lifting-Line Theory for Arbitrarily Shaped Wings

M. L. Rasmussen* and D. E. Smith†
University of Oklahoma, Norman, Oklahoma 73019-1052

This paper presents a new method for solving the classical lifting-line equation. The spanwise lift (or circulation) distribution is to be determined when the spanwise chord distribution and spanwise twist distribution are resolved separately and arbitrarily into their Fourier-series representations. An infinite set of equations for the resulting circulation Fourier-series coefficients is obtained in terms of the Fourier coefficients for the wing-chord shape and the twist distribution. When the equations are expressed in matrix form, the contributions of planform shape and twist are readily perceived. The set of equations can be truncated arbitrarily for the first N number of unknown coefficients, and easily solved by various software packages. Convergence properties can then be readily established by examining changes associated with changes in levels of truncation. A five-by-five ($N = 5$) truncation system is found to be sufficient for a wide variety of problems. Several example problems are considered, and the results are compared. The new method converges faster and is more accurate for the same level of truncation. Moreover, in comparison with other methods, it is comprehensive, rigorous, and lends itself to insight regarding the interactions of lift distribution, planform shape, and twist.

Introduction

CLASSICAL lifting-line theory forms the foundation for aerodynamic design. In addition to furnishing a computational means, it provides the conceptual basis for understanding wing theory and flight itself. Although lifting-surface theory is now used to carry out calculations with great accuracy, lifting-line theory is still utilized for rapid estimation of spanwise load distributions and the basic aerodynamics of straight wings. A great deal has been said and done regarding the mathematical analysis of the basic lifting-line equation. Nevertheless, the many proposed methods of determining the lift distribution for a given wing shape with a given geometric and aerodynamic twist, when viewed from a comprehensive basis, have shortcomings that stem from either conceptual or practical considerations, or both. The objective of this paper is to produce a new analysis that alleviates some of these shortcomings. After a brief background discussion, a comprehensive scheme will be generated that is accurate, practical, and lends itself to a better understanding of how the wing shape and twist contribute to the lift (or circulation) distribution.

Lifting-line theory is formulated in terms of a singular integral equation that relates the spanwise circulation distribution with the spanwise shape of the wing and the geometric and aerodynamic twist of the wing along its span. The indirect problem is easier to calculate; the circulation distribution is specified, and either the chord distribution or the twist distribution is to be determined when the other is given. The direct problem is more difficult to calculate; here, the spanwise shape of the wing and the twist are specified, and the circulation distribution is to be determined. It is to this latter problem that we primarily direct our attention.

The classical lifting-line theory is usually attributed to Prandtl. An interesting historical perspective can be found in Anderson.[1] Discussions of some of the many methods used to deal with the lifting-line equation can be found in the books by Bisplinghoff et al.,[2] Robinson and Laurmann,[3] Thwaites,[4] and Schlichting and Truckenbrodt.[5] The most popular schemes for solving the lifting-line equation have been collocation methods. In these schemes, a finite sine series for the circulation distribution is assumed, and the coefficients of the terms in the series are determined by requiring the lifting-line equation to be satisfied identically at a number of locations along the span, equal to the number of terms in the series. Enough terms and stations are taken to presumably provide adequate convergence. A straightforward scheme was popularized by Glauert,[6] and a more accurate scheme based on Gaussian quadratures was put forth by Multhopp.[7] One of the difficulties with collocation schemes is that, unless the collocation points are clustered in such a way that they capture any sudden changes in wing characteristics, a given set of collocation points may describe more than one wing. To this degree, the methods are arbitrary and nonunique. Nevertheless, the methods are widely used; the method of Glauert in particular is widely used in modern textbooks[8–10] to demonstrate basic results for finite wing aerodynamics.

Another class of approximate methods can be classified as variational methods.[11–13] These methods do not depend on a finite number of isolated collocation points along the wing as for collocation schemes, but allow for an approximate solution along the entire span. The roles of planform shape and twist are not explicitly exhibited, but are bound up with weighted integrals over their respective functions evaluated over the span. The variational methods have not met with popular usage.

A particular method of interest is that of Lotz[14] and Karamcheti,[15] who expanded the twist distribution in a conventional Fourier series, but the chord function was expanded in a Fourier series in terms of its inverse. Although this allowed for a rational analysis and a solution for the circulation distribution, the inverse nature of the chord resolution does not lend itself to practical usage. (The forthcoming new analysis will be similar, but the chord function will be expanded directly in a conventional Fourier series.)

The foregoing methods all involve a linear set of simultaneous algebraic equations for the coefficients of the sine-series representation for the circulation. In the days before digital computers, solving these equations was extremely laborious. This gave rise to a number of simplified semiempirical approximate methods, perhaps the most notable of which is from Schrenk.[16] Although now outmoded, Schrenk's method is still referred to because of its utility and historical interest.

Received July 6, 1998; revision received Sept. 16, 1998; accepted for publication Sept. 21, 1998.

*Professor, Aerospace and Mechanical Engineering, 1325 Brookhaven Boulevard. Associate Fellow AIAA.

†Associate Professor, Aerospace and Mechanical Engineering, 1325 Brookhaven Boulevard. Member AIAA.

A number of alternatives to dealing directly with the classical lifting-line equation also exist. Laporte[17] found exact solutions for the spanwise lift distribution for a certain class of wing shapes. Van Dyke[18] and Ashley and Landahl[19] approached the lifting-line theory as a singular-perturbation problem, valid for the large aspect ratios, and obtained a number of interesting theoretical results.

There are also purely numerical approaches to solving the lifting-line problem, geared to the digital computer. A finite difference scheme has been developed by Anderson[1] and Anderson et al.,[20] which is particularly useful for including nonlinear effects. A numerical model is also given by McCormick.[21]

The forthcoming new analysis for solving the classical lifting-line equation is based on a rigorous Fourier-series analysis, where the arbitrary shape of the wing and the twist are represented explicitly, and the lift distribution (or circulation) is obtained explicitly in terms of the Fourier coefficients for the chord and twist distribution. The comprehensive results of the analysis are obtained once and for all, and do not depend on an arbitrary distribution of collocation points. An infinite set of algebraic equations is obtained for the circulation coefficients, which must be truncated arbitrarily for a desirable degree of convergence. A number of the numerical results are obtained that illustrate different wing shapes and rates of convergence, and comparisons are made with the corresponding collocation method of Glauert.[6] The new method is accurate, converges rapidly, is comprehensive, and provides more insight as to how the circulation distribution depends on the shape of the wing and the twist distribution.

Here we summarize the derivation of the classical lifting-line integral equation, the details of which can be found in various of the texts appearing in the list of references. The local airfoil-section lift coefficient is given by

$$c_l = m_o(\alpha - \alpha_{0L} - \alpha_i) \tag{1}$$

where α is the geometric angle of attack of the section chord line relative to the freestream, α_{0L} is the angle of attack at zero lift for the local airfoil section (determined essentially by the local camber line shape for thin airfoils), and α_i is the angle of attack induced by the trailing vortex sheet. The section lift-curve slope is denoted by m_o, which for thin-airfoil theory is given by $m_o = 2\pi$. In general, all of the variables in Eq. (1) are functions of y, the location along the span, as indicated in Fig. 1. The section lift coefficient is given by

$$c_l = \frac{L'(y)}{1/2\rho V_\infty^2 c(y)} = \frac{2\Gamma(y)}{V_\infty c(y)} \tag{2}$$

where $c(y)$ is the chord of the airfoil section at the position y, and the Kutta–Joukowski law, $L' = \rho V_\infty \Gamma$, has been used to introduce the circulation Γ. The induced angle of attack can be expressed as an integral over the circulation distribution[9]:

$$\alpha_i(y) = \frac{1}{4\pi V_\infty} \int_{-b/2}^{b/2} \frac{d\Gamma(y_o)}{y - y_o} \tag{3}$$

where b is the wingspan. When Eqs. (2) and (3) are substituted into Eq. (1), the fundamental integral–equation relation between $\Gamma(y)$, $\alpha(y) - \alpha_{0L}(y)$, and $c(y)$ is obtained.

A common means for analyzing the fundamental integral equation is to change the variables from y to θ, such that $y = (b/2)\cos\theta$, and then to assume a sine-series representation for $\Gamma(\theta)$:

$$\Gamma(\theta) = \frac{1}{2} m_{or} c_r V_\infty \sum_{n=1}^{\infty} A_n \sin n\theta \tag{4}$$

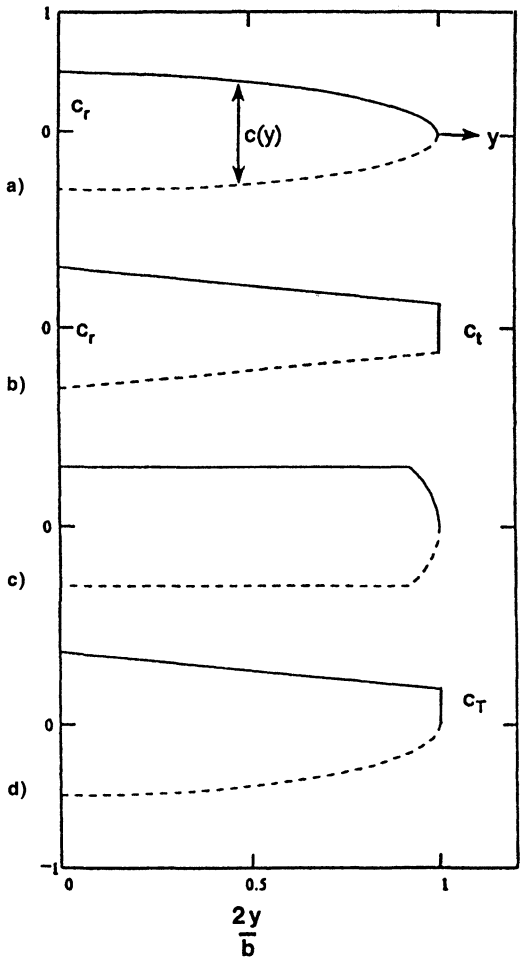

Fig. 1 Planform Shapes and notation (semispans): a) elliptic wing, b) tapered wing, c) rectangular wing with rounded tips, and d) pseudo-Thunderbolt wing.

where m_{or} and c_r are the values of m_o and c evaluated at the root chord, $y = 0$ or $\theta = \pi/2$. Here, we will assume that the load distribution on the right–left sides of the wing is symmetric, and hence, only odd values of n will be considered. If the function $\Gamma(\theta)$ is known over the interval $0 \leq \theta \leq \pi$, and if the sine series is truncated at a finite number of terms N, then the N coefficients A_n can be determined by a collocation method at an arbitrary selected N number of positions in the interval $0 < \theta \leq \pi/2$ (for symmetric loadings). On the other hand, the N coefficients can also be evaluated by the Euler formula:

$$A_n = \frac{4}{\pi} \int_o^{\pi/2} \frac{2\Gamma(\theta)}{m_{or} c_r V_\infty} \sin n\theta \, d\theta \tag{5}$$

This also holds for an infinite number of terms, in which case the sine series is officially a Fourier series. It can be shown that for a finite series, use of the Euler formula as opposed to an arbitrary collocation method leads to the minimum error in the least-square sense.

When Eq. (4) is used to evaluate the integral in Eq. (3), together with Glauert's integral formula,[6,9] there results

$$\alpha_i = \frac{m_{or} c_r}{4b} \sum_{n=1}^{\infty} n A_n S_n(\theta) \tag{6}$$

where

$$S_n(\theta) \equiv \sin n\theta / \sin\theta \tag{7}$$

When Eqs. (4) and (6) are used in Eq. (1), Eq. (1) can be rewritten as

$$\frac{m_o}{m_{or}}\frac{c(\theta)}{c_r}\left[\alpha_a(\theta) - \frac{m_{or}c_r}{4b}\sum_{n=1}^{\infty} nA_nS_n(\theta)\right] = \sum_{n=1}^{\infty} A_n \sin n\theta \quad (8)$$

where

$$\alpha_a \equiv \alpha - \alpha_{0L} \quad (9)$$

is referred to as the absolute angle of attack. The variation of α_a along the span is the twist, the variation in α is the geometric twist, and the variation in α_{0L} is the aerodynamic twist. The sine-series representation for the circulation $\Gamma(\theta)$ has converted the integral–equation formulation into a trigonometric-series representation [Eq. (8)]. If the sine-series coefficients A_n are taken as given, i.e., by a Fourier-series representation, then either $c(\theta)/c_r$ or $\alpha_a(\theta)$ can be determined when the other is given together with m_o/m_{or} (the indirect problem). On the other hand, if $c(\theta)/c_r$ and $\alpha_a(\theta)$ are given (the direct problem), determining the set of sine-series coefficients A_n is a more complicated procedure. This is commonly done by one of several methods of collocation analyses. The object of the paper is to present an alternative Fourier-series analysis, which is less arbitrary, more general, and leads to more theoretical insights.

Before the Fourier analysis is undertaken, there are several additional formulas that need to be recorded. The overall lift coefficient is determined by

$$C_L = \frac{2}{V_\infty S}\int_{-b/2}^{b/2} \Gamma\, dy = \frac{\pi m_{or}c_r b}{4S} A_1 \quad (10)$$

where S is the planform area of the wing. Thus, the lift coefficient C_L depends only on the first coefficient A_1. Correspondingly, it can be shown that the induced drag coefficient is given by the well-known result

$$C_{D_i} = (C_L^2/\pi \mathrm{AR})(1 + \delta) \quad (11)$$

where $\mathrm{AR} \equiv b^2/S$ is the aspect ratio and

$$\delta \equiv \sum_{n=3}^{\infty} n\left(\frac{A_n}{A_1}\right)^2 \quad (12)$$

for the symmetric load distribution. The factor δ is never negative. It is zero, and thus, a minimum for the elliptic load distribution. The value of δ is thus a measure of the differences in induced drag among various wing configurations.

It is useful to introduce a factor τ for the lift coefficient that corresponds to expression (11) for the induced-drag coefficient. Toward this end, we define τ in a conventional way by means of the formula

$$C_L = \frac{m_{or}\alpha_o}{1 + (m_{or}/\pi \mathrm{AR})(1 + \tau)} \quad (13)$$

where α_o is the average of the absolute angle of attack α_a for a twisted wing. One can solve for τ in terms of A_1 by setting Eqs. (10) and (13) equal, and obtain

$$\tau = \frac{\pi \mathrm{AR}}{m_{or}}\left(\frac{4}{\pi}\frac{S}{bc_r}\frac{\alpha_o}{A_1} - 1\right) - 1 \quad (14)$$

For an elliptic load distribution and zero twist, which corresponds to an elliptic chord distribution, the factor τ is zero. Thus, τ is also a measure of differences, related to lift, among various wing configurations. The factors τ and δ were utilized by Glauert[6] to represent aerodynamic differences in tapered wings with variations in aspect and taper ratios.

Fourier-Series Analysis

A general solution for the basic lifting-line equation [Eq. (8)] will now be devised in terms of Fourier-series representations for the chord and twist distributions. The spanwise distribution of the planform shape, $c = c(y)$, can be represented in terms of the angle θ by making the substitution $y = (b/2)\cos\theta$. The Fourier sine-series representation can then be made

$$\frac{c(\theta)}{c_r} = \sum_{n=0}^{\infty} C_{2n+1} \sin(2n + 1)\theta \quad (15)$$

where only odd terms are taken to account for right–left symmetry, and

$$C_{2n+1} \equiv \frac{4}{\pi}\int_0^{\pi/2} \frac{c(\theta)}{c_r} \sin(2n + 1)\theta\, d\theta, \qquad n = 0, 1, 2, 3, \ldots \quad (16)$$

The planform area S is

$$S = \int_{-b/2}^{b/2} c(y)\, dy = \frac{b}{2}\int_0^{\pi} c(\theta)\sin\theta\, d\theta = \frac{\pi b c_r}{4} C_1 \quad (17)$$

Thus, only the first term of the series determines the planform area.

The spanwise distribution of the absolute angle of attack $\alpha_a(\theta)$ (twist) can be represented by a Fourier cosine series (with even terms for right–left symmetry):

$$\alpha_a(\theta) = \sum_{n=0}^{\infty} a_{2n} \cos 2n\theta \quad (18a)$$

where a_o is the average angle of attack α_o

$$\alpha_o \equiv a_o = \frac{2}{\pi}\int_o^{\pi/2} \alpha_a(\theta)\, d\theta \quad (18b)$$

$$a_{2n} = \frac{4}{\pi}\int_o^{\pi/2} \alpha_a(\theta)\cos 2n\theta\, d\theta, \qquad n = 1, 2, 3, \ldots \quad (18c)$$

Now consider the function $S_n(\theta)$ for odd values of n, defined by Eq. (7). We note that

$$S_1 = 1, \qquad S_3 = 1 + 2\cos 2\theta$$
$$S_5 = 1 + 2\cos 2\theta + 2\cos 4\theta \quad (19)$$
$$S_{2n+1} = 1 + 2\sum_{m=1}^{n} \cos 2m\theta, \qquad n = 1, 2, 3, \ldots$$

Taking expressions (19) into account, we can write the induced angle of attack as a Fourier cosine series:

$$\frac{4b}{m_{or}c_r}\alpha_i = \sum_{n=0}^{\infty} (2n + 1)A_{2n+1}S_{2n+1} = \sum_{n=0}^{\infty} B_{2n}\cos 2n\theta \quad (20a)$$

where

$$B_o \equiv \sum_{m=0}^{\infty} (2m + 1)A_{2m+1}$$
$$B_{2n} \equiv 2\sum_{m=n}^{\infty} (2m + 1)A_{2m+1}, \qquad n = 1, 2, 3, \ldots \quad (20b)$$

With the preceding notations and definitions, the fundamental lifting-line equation [Eq. (8)] can be written

$$\frac{m_o}{m_{or}}\left[\sum_{k=0}^{\infty} C_{2k+1}\sin(2k+1)\theta\right]\left[\sum_{s=0}^{\infty}\left(a_{2s}-\frac{m_{or}c_r}{4b}B_{2s}\right)\cos 2s\theta\right]$$
$$=\sum_{n=0}^{\infty} A_{2n+1}\sin(2n+1)\theta \qquad (21)$$

It is useful to normalize the coefficients by further definitions. Let

$$a_o^* = 1, \qquad a_{2n}^* = \frac{a_{2n}}{a_o}, \qquad n = 0, 2, 3, \ldots$$
$$C_1^* = 1, \qquad C_{2n+1}^* = \frac{C_{2n+1}}{C_1}, \qquad n = 0, 2, 3, \ldots$$
$$A_{2n+1}^* = \frac{A_{2n+1}}{C_1\alpha_o}, \qquad n = 0, 2, 3, \ldots \qquad (22)$$
$$B_o^* = \sum_{m=0}^{\infty}(2m+1)A_{2m+1}^*$$
$$B_{2n}^* = 2\sum_{m=n}^{\infty}(2m+1)A_{2m+1}^*, \qquad n = 1, 2, 3, \ldots$$

In addition, let us assume that m_o is the same at every spanwise location, i.e., $m_o = m_{or}$. Then Eq. (21) can be written

$$\left[\sum_{k=0}^{\infty} C_{2k+1}^*\sin(2k+1)\theta\right]\left[\sum_{s=0}^{\infty}\left(a_{2s}^*-\frac{m_o}{\pi\mathrm{AR}}B_{2s}^*\right)\cos 2s\theta\right]$$
$$=\sum_{n=0}^{\infty} A_{2n+1}^*\sin(2n+1)\theta \qquad (23)$$

where use has been made of expression (17) for C_1. In this notation, factor τ from expression (14) can be expressed as

$$\tau = (\pi\mathrm{AR}/m_o)[(1/A_1^*) - 1] - 1 \qquad (24)$$

When the Fourier chord-distribution coefficients C_{2n+1}^* and the Fourier twist-distribution coefficients a_{2n}^* have been specified, then the circulation coefficients A_{2n+1}^* can be determined from Eq. (23) in terms of the parameter $m_o/(\pi\mathrm{AR})$. The aerodynamic parameters τ and δ can then be immediately determined.

The product of the sine series and the cosine series on the left side of Eq. (23) can be resolved into a single sine series by use of the trigonometric identity:

$$\sin(2k+1)\theta\cos 2s\theta = \tfrac{1}{2}[\sin(2k+1+2s)\theta + \sin(2k+1-2s)\theta] \qquad (25)$$

After the sine terms are collected on the left side of Eq. (23), the respective coefficients of each term of $\sin(2n+1)\theta$ on the left and right sides can be equated. The results are

$$\frac{1}{2}\left\{a_o^*C_{2n+1}^* + \sum_{k=0}^{\infty}[a_{|n-k|}^* - a_{2(n+k+1)}^*]C_{2k+1}^*\right\} - \frac{1}{2}\frac{m_o}{\pi\mathrm{AR}}$$
$$\times\left\{B_o^*C_{2n+1}^* + \sum_{k=0}^{\infty}[B_{2|n-k|}^* - B_{2(n+k+1)}^*]C_{2k+1}^*\right\} = A_{2n+1}^*$$
$$n = 0, 1, 2, 3, \ldots \qquad (26)$$

Recall from Eqs. (22) that the coefficients B_{2n}^* contain the coefficients A_{2n+1}^*. If the circulation coefficients A_{2n+1}^* and the twist coefficients a_{2n}^* are known (the indirect problem), then Eqs. (26) constitute an infinite set of linear equations for the planform-shape coefficients C_{2n+1}^*.

For the direct problem, the A_{2n+1}^* can be separated out in Eqs. (26), and like terms collected. When this is done, the result can be cast in the form

$$\sum_{n=0}^{\infty} C_{(2m+1)(2n+1)}A_{2n+1}^* = D_{2m+1}, \qquad m = 0, 1, 2, 3, \ldots \qquad (27a)$$

where

$$C_{(2m+1)(2n+1)} \equiv \delta_{(2m+1)(2n+1)} + \frac{(2n+1)m_o}{\pi\mathrm{AR}}\sum_{k=|m-n|}^{m+n} C_{2k+1}^*$$
$$m, n = 0, 1, 2, 3, \ldots \qquad (27b)$$

$$D_{2n+1} \equiv \frac{1}{2}\left\{a_o^*C_{2n+1}^* + \sum_{k=0}^{\infty}[a_{2|n-k|}^* - a_{2(n+k+1)}^*]C_{2k+1}^*\right\}$$
$$n = 0, 1, 2, 3, \ldots \qquad (27c)$$

and $\delta_{(2m+1)(2n+1)}$ is the Kroneker delta function. Equation (27a) constitutes an infinite set of equations for A_{2n+1}^*, when C_{2n+1}^* and a_{2n}^* are given, together with $m_o/(\pi\mathrm{AR})$. If only the first five equations are kept for the first five terms, the results can be displayed in the matrix form

$$\begin{bmatrix} C_{11} & C_{13} & C_{15} & C_{17} & C_{19} \\ C_{31} & C_{33} & C_{35} & C_{37} & C_{39} \\ C_{51} & C_{53} & C_{55} & C_{57} & C_{59} \\ C_{71} & C_{73} & C_{75} & C_{77} & C_{79} \\ C_{91} & C_{93} & C_{95} & C_{97} & C_{99} \end{bmatrix}\begin{bmatrix} A_1^* \\ A_3^* \\ A_5^* \\ A_7^* \\ A_9^* \end{bmatrix} = \begin{bmatrix} D_1 \\ D_3 \\ D_5 \\ D_7 \\ D_9 \end{bmatrix} \qquad (28)$$

The nature of the coefficients can be seen from the first several terms:

$$C_{11} = 1 + \frac{m_o}{\pi\mathrm{AR}}, \quad C_{13} = \frac{3m_o}{\pi\mathrm{AR}}C_3^*, \quad C_{15} = \frac{5m_o}{\pi\mathrm{AR}}C_5^*$$
$$C_{31} = \frac{m_o}{\pi\mathrm{AR}}C_3^*, \quad C_{33} = 1 + \frac{3m_o}{\pi\mathrm{AR}}(1 + C_3^* + C_5^*)$$
$$C_{35} = \frac{5m_o}{\pi\mathrm{AR}}(C_3^* + C_5^* + C_7^*), \quad C_{51}^* = \frac{m_o}{\pi\mathrm{AR}}C_5^*$$
$$C_{53} = \frac{3m_o}{\pi\mathrm{AR}}(C_3^* + C_5^* + C_7^*) \qquad (29)$$
$$C_{55} = 1 + \frac{5m_o}{\pi\mathrm{AR}}(1 + C_3^* + C_5^* + C_7^* + C_9^*)$$
$$D_1 = \left(1 - \frac{a_2^*}{2}\right)C_1^* + \frac{1}{2}(a_2^* - a_4^*)C_3^* \ldots\ldots$$
$$D_3 = \frac{1}{2}(a_2^* - a_4^*)C_1^* + \left(1 - \frac{a_6^*}{2}\right)C_3^* \ldots\ldots$$

It is not difficult to discern the remaining terms by extension and the use of Eqs. (27b) and (27c).

The coefficients of the square matrix in Eq. (28) are determined only by the wing planform shape, i.e., by the aspect ratio and the chord Fourier coefficients C_{2n+1}^*. The effects of twist appear in the column matrix on the right side of Eq. (28), which involves the Fourier coefficients C_{2n+1}^* also, but is independent of the aspect ratio. When there is no twist, the D_{2n+1} elements reduce to $D_{2n+1} = C_{2n+1}^*$. The elements of the square matrix and the right-side column matrix are fixed, depending on the wing shape and the twist. The level of approximation for the circulation coefficients A_{2n+1}^* depends on the size of the square matrix and corresponding right-side column matrix re-

tained. The elements of the matrices do not change with the level of truncation. This is in contrast to collocation methods, for which the elements and number of elements change according to the location and the number of collocation prints. For the present analysis, a five-by-five system, such as represented by Eq. (28), generally gives a good approximation for a variety of problems. This will be demonstrated by several example problems.

Certain features of wing characteristics can be gleaned from the analysis itself. As an example, consider solving for A_1^* from the first of Eqs. (27), in the form

$$A_1^* = D_1 \Big/ \left[1 + \frac{m_o}{\pi \mathrm{AR}} \left(1 + 3C_3^* \frac{A_3^*}{A_1^*} + 5C_5^* \frac{A_5^*}{A_1^*} + \cdots \right) \right] \tag{30}$$

Then the factor τ relating to the lift coefficient [Eq. (24)] can be expressed as

$$\tau = \frac{1}{D_1} \left[\sum_{n=3}^{\infty} n \frac{C_n}{C_1} \frac{A_n}{A_1} \right] + \left(\frac{1}{D_1} - 1 \right) \left(\frac{\pi \mathrm{AR}}{m_o} - 1 \right) \tag{31}$$

which holds for symmetric loading. This expression bears a resemblance to the parameter δ for the induced drag, given by Eq. (12). All of the effects of twist are contained in the parameters $D_1, D_3, D_5 \cdots$. When there is no twist, then $D_1 = C_1^* = 1$, and Eq. (31) reduces to an even stronger resemblance to Eq. (12) for δ. These and other aspects will be discussed further when specific examples are analyzed.

Example Problems

Several example problems will now be considered that demonstrate the utility, accuracy, and range of the analysis ($m_o = 2\pi$). First it is noted that the classical result for an untwisted elliptical wing is contained in the results (see Fig. 1a). In this case, we have $C_1 = 1$ and $C_3 = C_5 = C_7 = \cdots = 0$, $a_2 = a_4 = a_6 = \cdots = 0$, and

$$A_1^* = \frac{1}{1 + (2/\mathrm{AR})} \tag{32}$$

together with $A_3 = A_5 = A_7 = \cdots = 0$. It follows that $\tau = \delta = 0$. Thus, both the chord distribution and the circulation distribution are described by only the first term of each of their corresponding Fourier sine series. A wing with elliptic planform and twist will be considered later. First, several examples with no twist will be considered. All of the calculations were performed on a 486 personal computer with the software MATHCAD 5 Plus. Each inversion of the typical matrix equation, [Eq. (28)], took a matter of a second or two.

Tapered Wing

A straight tapered wing is described by (see Fig.1b)

$$\begin{aligned} c(y)/c_r &= 1 - (1 - \lambda)|2y/b| \\ c(\theta)/c_r &= 1 - (1 - \lambda)|\cos\theta| \end{aligned} \tag{33}$$

where $\lambda \equiv c_t/c_r$ is the taper ratio, and c_t is the chord at the tip. A rectangular wing is the special case described by $\lambda = 1$. The Fourier coefficients are given by

$$C_1 = \frac{2(1 + \lambda)}{\pi}$$

$$C_{2n+1} = \frac{4}{\pi} \left[\frac{1}{2n + 1} - \frac{1 - \lambda}{4} \frac{2n + 1 - (-1)^n}{n(n + 1)} \right]$$

$$n = 1, 2, 3, \ldots \tag{34}$$

Note that for a rectangular wing ($\lambda = 1$), the coefficients $C_{2n+1}^* = 1/(2n + 1)$ decrease monotonically. This may not be true, however, for certain tapered wings; we note that the first few coefficients for $n \neq 0$ are

$$C_3 = \frac{2}{\pi} \left(\lambda - \frac{1}{3} \right), \quad C_5 = \frac{2}{3\pi} \left(\lambda + \frac{1}{5} \right), \quad C_7 = \frac{2}{3\pi} \left(\lambda - \frac{1}{7} \right) \tag{35}$$

The coefficient C_3 vanishes when $\lambda = 1/3$. Thus, when λ is small enough, the coefficients C_{2nn} do not decrease monotonically. It is reasonable to expect that the circulation coefficients A_{2n+1} bear a correspondence to this behavior. Moreover, from a perusal of expressions (31) and (12) for τ and δ, it might be expected a priori that τ and δ would have a minimum for certain values of λ. This, in fact, is the case, as parametric calculations will illustrate.

We now wish to demonstrate the outcomes of the present analysis for various truncation levels of the infinite set of Eqs. (27a). We make the calculations for 4, 5, 6, 7, and 8 terms of the series. The matrix form of the 5-term series is illustrated by Eq. (28), with $D_{2n+1} = C_{2n+1}^*$ for zero twist. The 4-term series is a subset of this matrix equation, and the 6-, 7-, and 8-term series are extensions of it. The comparison of the common terms demonstrates the accuracy and the convergence rate of the analysis. The results of the present analysis will also be compared with a corresponding commonly used collocation method, generally attributed to Glauert.[6] The first case will be for a rectangular wing ($\lambda = 1$) and AR = 6, for which a 4-term series was used as an example by Kuethe and Chow.[9] The second case will be for a tapered wing ($\lambda = 0.4$) and AR = 9, for which a 4-term series was used by Bertin and Smith.[10] The details of the 4-term collocation method can be found in those references, as well as in von Mises[8] for other examples. In these examples, the collocation points are equally spaced such that $\Delta\theta = 90$ deg/n, where n is the number of terms retained in the sine series. For instance, for the 4-term series, the collocation points are located at $\theta = 22.5$, 45, 57.5, and 90 deg. The results for the rectangular wing are shown in Table 1, and the results for the tapered wing are shown in Table 2.

For the rectangular wing with AR = 6, all of the circulation coefficients $A_1^*, A_3^*, A_5^*, \ldots$ decrease monotonically. As seen from a perusal of Table 1 for the second term, A_3^*, the change

Table 1 Rectangular wing[a]

	Present analysis					Collocation analysis				
Coefficient	4-term	5-term	6-term	7-term	8-term	4-term	5-term	6-term	7-term	8-term
A_1^*	0.72127	0.72112	0.72108	0.72106	0.72105	0.72054	0.72084	0.72095	0.72099	0.72101
A_3^*	0.08828	0.08795	0.08785	0.08781	0.08779	0.08669	0.08736	0.08758	0.08767	0.08771
A_5^*	0.01948	0.01892	0.01877	0.01872	0.0187	0.01711	0.01812	0.01842	0.01854	0.01860
A_7^*	0.00718	0.00578	0.00553	0.00545	0.00542	0.00300	0.00467	0.00509	0.00528	0.00531
A_9^*	——	0.00286	0.00219	0.00206	0.00202	——	0.000957	0.00161	0.00181	0.00189
A_{11}^*	——	——	0.00136	0.00099	0.00092	——	——	0.00037	0.00066	0.00076
A_{13}^*	——	——	——	0.00073	0.00052	——	——	——	0.00016	0.00031
A_{15}^*	——	——	——	——	0.00043	——	——	——	——	0.000081
τ	0.1593	0.1602	0.1604	0.1605	0.1606	0.1635	0.1618	0.1612	0.1609	0.1608
δ	0.0493	0.0487	0.0485	0.0484	0.0483	0.0464	0.0475	0.0479	0.0481	0.0482

[a]AR = 6, $\lambda = 1$.

Table 2 Tapered wing[a]

	Present analysis					Collocation analysis				
Coefficient	4-term	5-term	6-term	7-term	8-term	4-term	5-term	6-term	7-term	8-term
A_1^*	0.81137	0.81076	0.81072	0.81061	0.81061	0.81610	0.81429	0.81322	0.81255	0.81209
A_3^*	0.01262	0.01168	0.01149	0.01135	0.01132	0.00363	0.00711	0.00865	0.00946	0.00994
A_5^*	0.04437	0.04223	0.04200	0.04172	0.04169	0.04254	0.04295	0.04280	0.04258	0.04239
A_7^*	0.00926	0.00702	0.00655	0.00622	0.00617	−0.00481	0.00151	0.00361	0.00452	0.00500
A_9^*	——	0.00910	0.00859	0.00793	0.00786	——	0.00763	0.00825	0.00828	0.00821
A_{11}^*	——	——	0.00197	0.00124	0.00112	——	——	−0.00218	−0.00072	−0.00010
A_{13}^*	——	——	——	0.00272	0.00258	——	——	——	0.00250	0.00257
A_{15}^*	——	——	——	——	0.00052	——	——	——	——	−0.00113
τ	0.0462	0.0504	0.0506	0.0514	0.0514	0.0140	0.0262	0.0335	0.0381	0.0413
δ	0.0166	0.0159	0.0155	0.0155	0.0152	0.0139	0.0150	0.0153	0.0154	0.0154

[a]AR = 9, λ = 0.4.

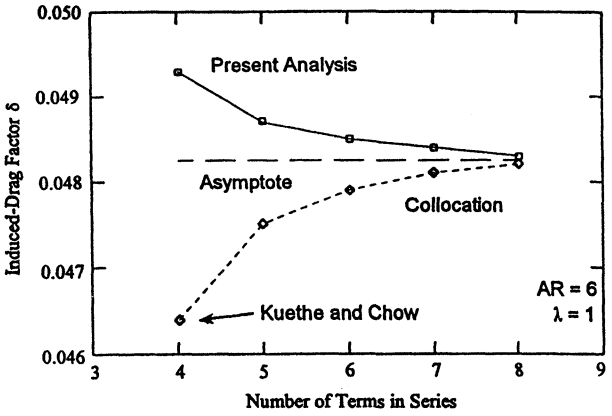

Fig. 2 Convergence properties of induced-drag factor δ for rectangular wing.

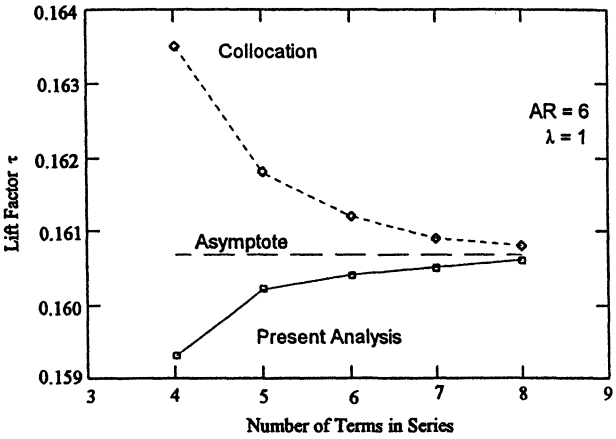

Fig. 3 Convergence properties of lift factor τ for tapered wing, λ = 0.4.

between the 4-term and the 8-term approximations is a decrease of 0.56% for the present analysis compared with a 1.2% increase for the collocation analysis, relative to the 8-term approximations. The corresponding values for the fourth coefficient, A_7^*, are a 32% decrease for the present analysis, and a 44% increase for the collocation analysis. Because the value of A_7^* is small, however, these errors are insignificant on the overall sine-series representation for Γ. The convergence properties for the induced-drag factor δ are shown in Fig. 2. The differences between the 4- and 8-term approximations are 2.1% for the present analysis, and 3.7% for the collocation analysis. The corresponding results for the lift factor τ are shown in Fig. 3. The differences between the 4- and 8-term approximations are 0.81% for the present method, and 1.7% for the collocation method. The 4-term result for δ obtained by the collocation method is the same as determined in Kuethe

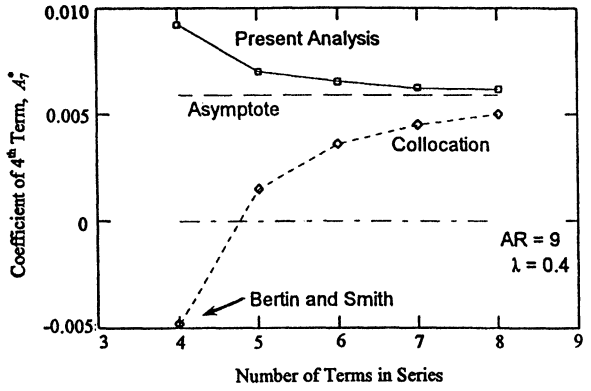

Fig. 4 Convergence properties of A_7^* for tapered wing, λ = 0.4.

and Chow.[9] The present method converges considerably faster and gives a better result for the same number of terms in the truncation approximation.

For the tapered wing, with λ = 0.4 and AR = 9, the sequence of circulation coefficients A_1^*, A_3^*, A_5^*, ... does not decrease monotonically as it does for the rectangular wing. The coefficients alternatively decrease and then increase, while getting smaller sequentially overall. This is consistent with the Fourier coefficients, C_{2n+1}, for the chord distribution, as can be seen from Eqs. (34) and (35). The leading every-other terms A_1^*, A_5^*, A_9^*, A_{13}^*, ... converge more rapidly than the smaller in-between terms A_3^*, A_7^*, A_{11}^*, ... The converging behavior of the second term, A_3^*, can established from Table 2. The 4-term approximation obtained by the collocation method is the same as that obtained by Bertin and Smith.[10] The changes between the 4- and 8-term approximations are an 11% decrease for the present analysis, and a 63% increase for the collocation method. The 5-term approximation for the present method differs by only 3.2% from the 8-term approximation. The convergence of the similarly behaving fourth term A_7^* is shown in Fig. 4. The differences between the 4- and 8-term approximations are 50% for the present method, and 196% for the collocation method. Notice that the 4-term approximation for A_7^*, according to the collocation, method is negative, which is consistent with the calculation of Bertin and Smith. The 5-term approximation differs from the 8-term approximation, according to the present analysis, by 14%. The term A_5^*, which is larger than its surrounding terms A_3^* and A_7^*, can be examined from Table 2. According to the present analysis, the value of A_5^* decreases sharply from the 4-term to the 5-term approximation. For the collocation method, A_5^* increases from the 4-term to the 5-term approximation, but then decreases steadily to the 8-term approximation without seeming to level off to an asymptotic value at this stage. Figure 5 shows the value of the lift factor τ as a function of the number of terms in the truncation series. The present method quickly converges, but the collocation method continues an increasing trend for τ, even for eight terms in the series. The induced-drag factor δ

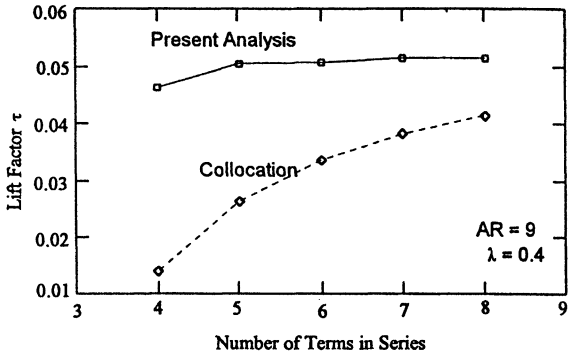

Fig. 5 Convergence properties of lift factor τ for tapered wing, $\lambda = 0.4$.

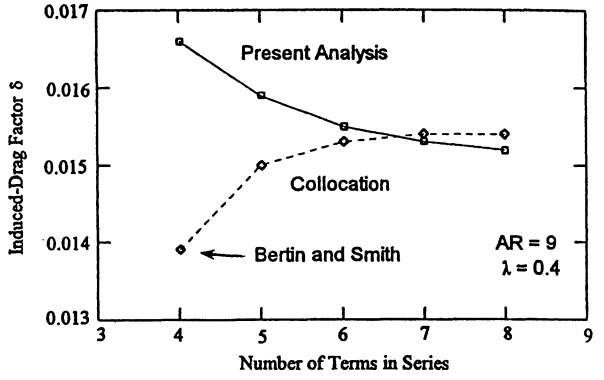

Fig. 6 Convergence properties of induced-drag factor δ for tapered wing, $\lambda = 0.4$.

is shown in Fig. 6. The result according to the present analysis decreases 9% from the 4-term to the 8-term approximation, which has nearly achieved its asymptotic value. The result of the collocation method increases 10% from the 4-term approximation to what appears to be an equilibrium value for the 8-term approximation, which is slightly above the result obtained for the present analysis. In view of the overall still-changing behavior of the collocation analysis, however, as exhibited in Fig. 4 and Table 2, it is possible that δ for the collocation method could undergo further changes as more terms in the series are retained.

Overall, the present method of analysis is seen to be superior to the collocation method. It gives better accuracy for the same number of terms in the truncation of the series, and it converges faster to an asymptotic value when more terms in the series are used. Aside from questions of numerical accuracy, the present method is rigorous in its approach, and can be readily used for systematic studies in a variety of ways, as will be demonstrated subsequently. The collocation method is not unique, that is, a given set of collocation points and values does not represent a unique planform shape. This aspect will be demonstrated shortly, and it can be strongly restrictive when aerodynamic control surfaces are taken into account by means of aerodynamic twist. The foregoing examples show that the 5-term series analyzed by the present method is accurate and robust. Its utility will be demonstrated by several more examples.

The induced-drag factor δ and the lift factor τ are shown in Figs. 7 and 8 as functions of the taper ratio λ for various values of the aspect ratio. For aerodynamic reasons, it is desirable that δ and τ be small, and it can be seen that δ and τ have minimums when λ is $\sim 1/3$. In this regard, it can be seen from Eq. (35) that the chord Fourier coefficient C_3 is zero when $\lambda = 1/3$. Both δ and τ increase when the AR increases for all values of λ. Strictly speaking, lifting-line theory is valid only for large ARs, and thus the curve for AR = 2 is shown only to indicate the spread of values for the smaller aspect ratios.

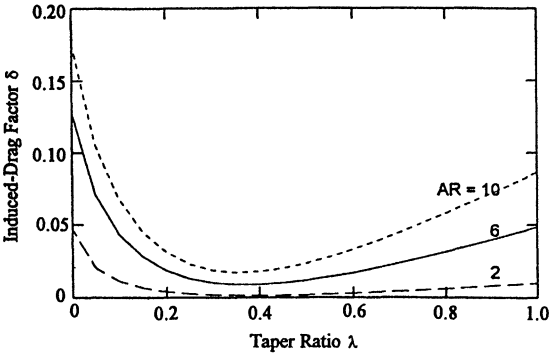

Fig. 7 Variation of induced-drag factor δ with taper ratio λ for tapered wings.

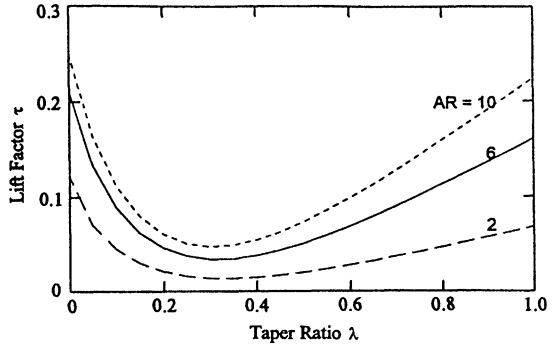

Fig. 8 Variation of lift factor τ with taper ratio λ for tapered wing.

Similar results to these, but less comprehensive, were calculated by Glauert,[6] using the 4-term collocation method. It should also be pointed out that the lift factor clearly depends on both the aspect ratio and the shape of the wing; a number of approximate formulas, such as reported in various of the listed references show a dependence on only AR.

The value of τ is generally larger than δ. The ratio has a maximum, where λ is somewhat larger than where τ and δ are minimums. For AR = 10, τ is nearly 10 times greater than δ, where τ/δ is a maximum.

Rectangular Wing with Rounded Tips

It is interesting to see the effect of rounding the tips of the tapered and rectangular wing. We consider the case of a rectangular wing with a rounded tip, as shown in Fig. 1c. We represent the wing shape by

$$\frac{c(\theta)}{c_r} = 1, \quad \theta_o \le \theta \le \pi - \theta_o = \frac{\sin\theta}{\sin\theta_o}, \quad \begin{cases} 0 \le \theta \le \theta_o \\ \pi - \theta_o \le \theta \le \pi \end{cases} \tag{36}$$

where $\cos\theta = 2y/b$. The shape shown in Fig. 1c corresponds to $\theta_o = 22.5$ deg or $2y/b = 0.924$. The four collocation points used earlier for the 4-term collocation method cannot capture the effect of this rounded tip, and thus, for this method the same results would be calculated for both the square-tip and rounded-tip rectangular wings for $\theta_o \le 22.5$ deg.

On the other hand, the Fourier coefficients for the chord distribution are

$$C_1 = \frac{2}{\pi}\left(\cos\theta_o + \frac{\theta_o}{\sin\theta_o}\right)$$

$$C_{2n+1} = \frac{4}{\pi}\left[\frac{\cos(2n+1)\theta_o}{2n+1} + \frac{(n+1)\sin 2n\theta_o - n\sin(2n+2)\theta_o}{4n(n+1)\sin\theta_o}\right], \quad n = 1, 2, 3, \ldots \tag{37}$$

Table 3 Rectangular wing with round tip[a]

θ_o	A_1^*	A_3^*	A_5^*	A_7^*	A_9^*	τ	δ
0 deg	0.72112	0.08795	0.01892	0.00578	0.00286	0.1602	0.0487
22.5 deg	0.73168	0.08248	0.01282	0.00052	−0.00188	0.1002	0.0397

[a]AR = 6.

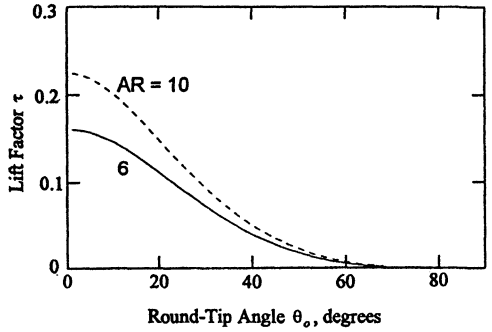

Fig. 9 Variation of lift factor τ for rectangular wings with rounded tips.

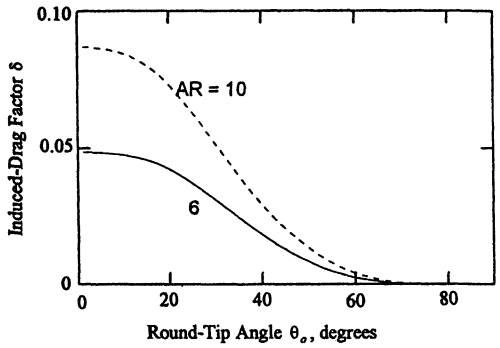

Fig. 10 Variation of induced-drag factor δ for rectangular wings with rounded tips.

Table 3 shows the first five of the circulation coefficients for AR = 6, based on the 5-term truncation, for $\theta_o = 0$ deg (square tip) and $\theta_o = 22.5$ deg (rounded tip). Except for A_1^*, all of the other coefficients decrease as θ_o becomes larger (when $\theta_o = 90$ deg, the elliptic wing is recovered). The lift factor τ and the induced-drag factor δ are reduced with wing-tip rounding. This is illustrated further in Figs 9 and 10, where τ and δ are shown as functions of θ_o for AR = 6 and 10. When θ_o increases to 70 deg, τ and δ have virtually been reduced to zero.

Pseudo-Thunderbolt Wing

The rectangular and tapered wings are of practical interest because of their ease and economy of construction, and the tapered wing has a low induced drag when λ is about 1/3. Another wing shape that might be of interest has a straight tapered leading edge, but a curved elliptic trailing edge (see Fig. 1d). This shape is reminiscent of the P-47 Thunderbolt wing. We describe this shape by

$$c(\theta)/c_r = \tfrac{1}{2}[1 - (1 - \lambda_T)|\cos\theta| + \sin\theta] \qquad (38)$$

where $\lambda_T = 2c_t/c_r$. The Fourier coefficients are

$$C_1 = \frac{1 + \lambda_T}{\pi} + \frac{1}{2}$$
$$C_{2n+1} = \frac{2}{\pi}\left[\frac{1}{2n+1} - \frac{1-\lambda_T}{4}\frac{2n+1-(-1)^n}{n(n+1)}\right], \quad n = 1, 2, 3, \ldots \qquad (39)$$

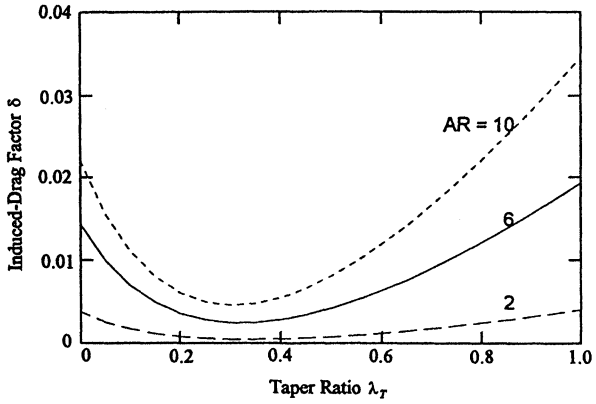

Fig. 11 Variation of induced-drag factor δ with taper ratio λ_T for pseudo-Thunderbolt wings.

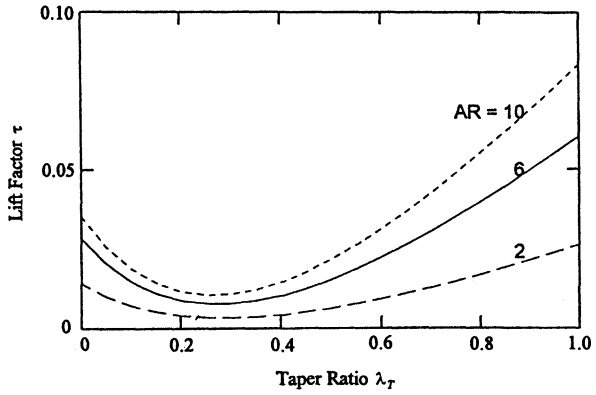

Fig. 12 Variation of lift factor τ with taper ratio λ_T for pseudo-Thunderbolt wings.

The coefficients C_3, C_5, ... are one-half of those given by Eq. (35) for the pure tapered wing, and $C_3 = 0$ for $\lambda_T = 1/3$. Figures 11 and 12 show the induced-drag factor δ and the lift factor τ plotted as functions of λ_T for various aspect ratios. Both δ and τ have minimums for λ_T slightly less than 1/3. The factors δ and τ for the Thunderbolt wing are smaller than for the wing with both tapered leading and trailing edges for the same value of AR and $\lambda = \lambda_T$.

The foregoing examples show the utility of the present method of dealing with various planform shapes in terms of the Fourier coefficients for the chord distribution along the span without twist. We now consider certain results that can be readily obtained involving twist.

Elliptic Wing with Twist

Consider a wing with an elliptic planform shape, such that $C_1 = 1$ and $C_3 = C_5 = C_7 = \ldots 0$. Then it is not difficult to obtain from Eqs. (27a) or (28) that the circulation coefficients are

$$A_1^* = \frac{1 - (a_2^*/2)}{1 + (2/\mathrm{AR})}$$
$$A_{2n+1}^* = \frac{a_{2n}^* - a_{2(n+1)}^*}{2\{1 + [2(2n+1)/\mathrm{AR}]\}}, \quad n = 1, 2, 3, \ldots. \qquad (40)$$

where a_{2n}^* are the Fourier coefficients for the twist distribution determined by Eqs. (18b) and (18c). This is an exact solution and is consistent with the results of Filotas.[22]

The case for a linear twist distribution is given by

$$\alpha_a = \alpha_r - (\alpha_r - \alpha_t)|\cos\theta| \tag{41}$$

where α_r and α_t are the absolute angles of attack at the root and at the tip, respectively. The Fourier coefficients are

$$\begin{aligned} a_o &= \alpha_r - (2/\pi)(\alpha_r - \alpha_t) \\ a_{2n} &= (4/\pi)(\alpha_r - \alpha_t)[(-1)^n/(4n^2 - 1)], \quad n = 1, 2, 3, \ldots \end{aligned} \tag{42}$$

The first four circulation coefficients can now be expressed as

$$\begin{aligned} A_1 &= \frac{\alpha_r - (4/\pi)[(\alpha_r - \alpha_t)/3]}{1 + (2/\mathrm{AR})}, \quad A_3 = -\frac{4}{\pi}\frac{\alpha_r - \alpha_t}{5[1 + (6/\mathrm{AR})]} \\ A_5 &= \frac{4}{\pi}\frac{\alpha_r - \alpha_t}{21[1 + (10/\mathrm{AR})]}, \quad A_7 = -\frac{4}{\pi}\frac{\alpha_r - \alpha_t}{45[1 + (14/\mathrm{AR})]} \end{aligned} \tag{43}$$

These results are in agreement with the numerical example computed by Katz and Plotkin[23] for AR = 6 and $\alpha_r = 0$. (Note the error in Katz and Plotkin and the evaluation of their equivalent of A_3.)

It is worth mentioning the special case of a quadratic twist distribution, given by

$$\begin{aligned} \alpha_a &= \alpha_r - (\alpha_r - \alpha_t)(2y/b)^2 \\ &= \alpha_r - (\alpha_r - \alpha_t)\cos 2\theta \\ &= a_o + a_2 \cos 2\theta \end{aligned} \tag{44}$$

where

$$a_o = (\alpha_r + \alpha_t)/2, \qquad a_2 = (\alpha_r - \alpha_t)/2 \tag{45}$$

Hence, the Fourier expansion for the twist involves only two terms, and the corresponding circulation expansion, [Eq. (40)], also amounts to only a two-term series. The results [Eqs. (42) and (45)], can both be used for general wing planform shapes.

Concluding Remarks

A new method has been presented for solving the classical lifting-line equation. The method is rigorous and based on Fourier-series expansions for the planform shape, twist distribution, and circulation distribution. The method converges faster and is more accurate for the same level of truncation than collocation methods. It is comprehensive and lends itself to systematic calculations and to a better understanding of the interacting parts of classical lifting-line theory. The method can be readily utilized for further systematic studies regarding the interactions of twist and wing shape, and their affects on load distributions and downwash distributions. In this regard, the new method is readily amendable to a study of flap deflections and locations, and does not require special analysis for the clustering of collocation points near the discontinuity edges of the flaps. The method can be extended to account for asymmetric wing loadings.

References

[1]Anderson, J. D., *Fundamentals of Aerodynamics*, 2nd ed., McGraw–Hill, New York, 1991.

[2]Bisplinghoff, R. L., Ashley, H., and Halfman, R. L., *Aeroelasticity*, Addison–Wesley, Reading, MA, 1955, pp. 229–238.

[3]Robinson, A., and Laurmann, J. A., *Wing Theory*, Cambridge Univ. Press, Cambridge, England, UK, 1956, Chap. 3.

[4]Thwaites, B., *Incompressible Aerodynamics*, Oxford Univ. Press, Oxford, England, UK, 1960.

[5]Schlichting, H., and Truckenbrodt, E., *Aerodynamics of the Airplane*, McGraw–Hill, New York, 1979, Chap. 3.

[6]Glauert, H., *The Elements of Aerofoil and Airscrew Theory*, 2nd ed., Cambridge Univ. Press, Cambridge, England, UK, 1959.

[7]Multhopp, H., "The Calculation of the Lift Distribution of Airfoils," British Ministry of Aircraft Production, R. T. P. 2392, translated from *Luftfahrtforschung*, Bd. 15, Nr. 14, 1938, pp. 153–169.

[8]Von Mises, R., *Theory of Flight*, Dover, New York, 1959, Chap. 3.

[9]Kuethe, A. M., and Chow, C.-Y., *Foundations of Aerodynamics*, 4th ed., Wiley, New York, 1986, Chap. 6.

[10]Bertin, J. A., and Smith, M. L., *Aerodynamics for Engineers*, 3rd ed., Prentice–Hall, Englewood Cliffs, NJ, 1998, Chap. 7.

[11]Gates, S. B., "An Analysis of a Rectangular Monoplane with Hinged Tips," Reports and Memoranda 1175, Aeronautical Research Committee, Aeronautical Research Council, London, 1928.

[12]Anderson, R. C., and Millsaps, K., "Application of the Galerkin Method to the Prandtl Lifting-Line Equation," *Journal of Aircraft*, Vol. 1, No. 3, 1964, pp. 126–128.

[13]Bera, R. J., "Some Remarks on the Solution of the Lifting-Line Equation," *Journal of Aircraft*, Vol. 11, No. 10, 1974, pp. 647, 648.

[14]Lotz, I., "Berechnung der Auftriebsverteilug beliebig geformter Flugel," *Zeitschrift für Flugtechnik und Motorluftschiffahrt*, Vol. 22, No. 7, 1931, pp. 189–195.

[15]Karamcheti, K., *Ideal-Fluid Aerodynamics*, Wiley, New York, 1966, Chap. 19.

[16]Schrenk, O., "A Simple Approximation Method for Obtaining the Spanwise Lift Distribution," NACA TM 948, translated from *Luftwissen*, Bd. 7, Nr. 4, 1940, pp. 118–130.

[17]Laporte, O., "Rigorous Solutions for the Spanwise Lift Distribution of a Certain Class of Airfoils," *Quarterly of Applied Mathematics*, Vol. 2, No. 3, 1944, pp. 232–250.

[18]Van Dyke, M. D., "Lifting-Line Theory as a Singular-Perturbation Problem," *Archiwum Mechaniki Stosowanej*, Vol. 16, No. 3, 1964, pp. 601–614.

[19]Ashley, H., and Landahl, M., *Aerodynamics of Wings and Bodies*, Addison–Wesley, Reading, MA, 1965, Chap. 7.

[20]Anderson, J. D., Corda, S., and VanWie, S. M., "Numerical Lifting-Line Theory Applied to Drooped Leading-Edge Wings Below and Above Stall," *Journal of Aircraft*, Vol. 17, No. 12, 1980, pp. 898–904.

[21]McCormick, B. W., *Aerodynamics, Aeronautics, and Flight Mechanics*, 2nd ed., Wiley, New York, 1995.

[22]Filotas, L. T., "Solution of the Lifting-Line Equation for Twisted Elliptic Wings," *Journal of Aircraft*, Vol. 8, No. 10, 1971, pp. 835, 836.

[23]Katz, J., and Plotkin, A., *Low-Speed Aerodynamics*, McGraw–Hill, New York, 1991, Chap. 8.